13th International ASTM/ESIS Symposium on Fatigue and Fracture Mechanics, (39th National Symposium on Fatigue and Fracture Mechanics), Jacksonville, Florida

THREE DIMENSIONAL NUMERICAL SIMULATION AND CHARACTERIZATION OF CRACK GROWTH IN THE WELD REGION OF A FRICTION STIR WELDED STRUCTURE

Banavara R. Seshadri [1], Stephen W. Smith [2] and John A. Newman [2]
NASA Langley Research Center
Hampton, Virginia

Extended Abstract

Friction stir welding (FSW) fabrication technology is being adopted in aerospace applications. The use of this technology can reduce production cost, lead-times, reduce structural weight and need for fasteners and lap joints, which are typically the primary locations of crack initiation and multi-site fatigue damage in aerospace structures. FSW is a solid state welding process that is well-suited for joining aluminum alloy components; however, the process introduces residual stresses (both tensile and compressive) in joined components. The propagation of fatigue cracks in a residual stress field and the resulting redistribution of the residual stress field and its effect on crack closure have to be estimated. To insure the safe insertion of complex integral structures, an accurate understanding of the fatigue crack growth behavior and the complex crack path process must be understood. A life prediction methodology for fatigue crack growth through the weld under the influence of residual stresses in aluminum alloy structures fabricated using FSW will be detailed. The effects and significance of the magnitude of residual stress at a crack tip on the estimated crack tip driving force are highlighted. The location of the crack tip relative to the FSW and the effect of microstructure on fatigue crack growth are considered. A damage tolerant life prediction methodology accounting for microstructural variation in the weld zone and residual stress field will lead to the design of lighter and more reliable aerospace structures.

Introduction

Friction Stir Welding (FSW) is a high potential joining technology for use in aerospace applications. Welding generally offers a reduction in production costs, lead-times, and a decrease of structural weight. FSW is a solid-state process; this makes it more effective to weld high strength aluminum alloys such as AA2024 and AA7075 that are prone to oxidation during fusion welding processes. The low process temperatures, with a maximum below solidus temperature, yield minimal reduction in strength. Furthermore, FSW is a robust process without emission of hazardous gasses or radiation which requires protection. In general, three zones can be distinguished in the weld, the stirred zone (nugget), the Thermo-Mechanically Affected Zone (TMAZ), and the Heat Affected Zone (HAZ). All three zones have different thermodynamic and/or mechanical history. To use FSW to manufacture an airworthy and damage tolerant structure, the fatigue behavior, including fatigue crack initiation, fatigue crack growth and residual strength [1], must be fully understood. Since the three weld zones influence the static and dynamic behavior of the joint differently, full

[1] Senior Research Scientist, National Institute of Aerospace, Hampton, VA.
[2] Senior Materials Research Engineer, Durability, Damage Tolerance & Reliability Branch.

understanding of the static and dynamic response of each individual zone is required. The goal of this research is to develop an advanced life prediction methodology which can be applied to advanced additive manufacturing technologies where the residual stress field is induced along with a gradient material microstructure in the FSW zone.

Finite Element Analyses

Many investigators have shown that residual stresses affect the fatigue life of materials [2-3]. It has been shown by Wohlfahrt and Lieurade [4] in an overview, that the change in stress-ratio (R) introduced by residual stress due to welding is directly correlated with a change in fatigue crack growth rate. Because the fatigue process is governed by conditions near the crack tip (e.g. stresses, strains), the residual stress field in the vicinity of the crack tip has been shown to be a major factor affecting the fatigue crack propagation (FCP) process (see Fig. 1). The magnitude and re-distribution of the residual stress field during crack extension must be known with reasonable accuracy to make reliable predictions of the effect of residual stress on the FCP process. Thus, if the equilibrated residual stress field is known then quantities such as the stress intensity factor at each crack location due to the presence of residual stresses, K_{res}, can be computed. Few techniques using the weight function method [5-6], experimental method [7-8] or finite element analysis using least square technique [9-11] have been presented in the literature. Extra precaution has to be taken while porting experimental data into FEM models [10-11]. The experimental data will not be in self-equilibrium leading to an erroneous FEM representation of the residual stress field [10-11]. Neutron diffraction has been used for measurement of residual stresses in various types of materials [12] and specimen types [13-14]. Liljedahl et al. [13-15] measured the stress distribution using a neutron diffraction technique and applied this measured distribution as the initial stress state in an FE model and allowed the stress to equilibrate. The resulting stress distribution in both middle tension M(T) and compact tension C(T) specimens [13-14] were compared with experimental data. As expected, the changes in the residual stresses predicted computationally are small compared to experimental data as an equilibrium solution is difficult to obtain. To overcome the difficulty associated with these models, the authors have used a new methodology based on equivalent thermal load to represent the residual stress field associated with the welding process. The thermal loads are calculated by defining initial strain due to welding along the length/width of the weld region. By knowing the elastic modulus, E, coefficient of thermal expansion, α and change in temperature, ΔT, equivalent thermal loads due to the residual stress field can be easily calculated (Fig. 2). The advantage of this methodology is that the residual stress field is always in self-equilibrium and the solution converges very fast. For the given welding process, the parameter, ΔT is calibrated by comparing with coupon generated data. Once calibrated, the same ΔT can used to generate the residual stress field for any other specimen type, component or panel of any size and shape containing a weld produced in the same manner. In the subsequent sections, the results from the proposed numerical methodology have been compared with experimental data independently generated at NASA Langley, Alcoa Technical Center and Fracture Technology Associates (FTA).

Results and Discussions

The comparison of both residual stress field and stress intensity factor solution for three mechanical test specimen configurations containing friction stir welds (Fig. 3) are made with experimental data. C(T) and M(T) mechanical test specimens are machined from a 1-inch thick AA 2024-T351 plate that was milled to remove ¼-inch from the top and bottom surfaces, sectioned into three parts and joined with two friction stir welds. The plate is milled

again to remove 1/8-inch from the top and bottom surfaces prior to machining the mechanical test specimens. The milling of the top and bottom surfaces is an attempt to produce fairly uniform residual stresses through the thickness of the plate to make the problem nominally two dimensional. The experimental data are generated using a slitting compliance method [16] at Alcoa Technical Center and a crack compliance method adapted from Donald and Lados [17] at NASA Langley and FTA. Numerical studies have been carried out in the past using both two and three-dimensional finite element analyses to obtain linear elastic fracture mechanics (LEFM) based stress intensity factor solutions for standard geometries under a mode I and II type of loading. Some of the most popular techniques used are virtual crack closure technique (VCCT) [18-20] and J-integral [21]. The virtual crack closure technique was proposed for 2D crack configuration by Rybicki and Kanninen [18] and was extended to three dimensions (3D-VCCT) by Shivakumar et al. [19]. In the current study, the 3D-VCCT technique has been used to generate stress intensity factor (SIF) solutions.

Comparison of residual stress field and stress intensity factor (SIF) solutions

A C(T) specimen exhibits two planes of symmetry, and consequently only one fourth of the geometry is required for modeling. Eight-node brick elements were used in the model. All analyses were for a 0.25 inch thick (B) specimen and 4.0 inch wide C(T) specimen. A typical ZIP3D [20] finite element model of the C(T) specimen is shown in Fig. 4. Aluminum alloy 2024-T3 was considered for all analyses with a modulus E = 10,000 ksi and the material behavior is elastic. The co-efficient of thermal expansion of the material is 13.0×10^{-6} deg F^{-1}. The residual stress profile for the C(T) specimen configuration labeled as tensile in Fig. 3 was determined for various values of ΔT and compared to the residual stress profile measured using the slitting compliance method (see Fig. 5a). A change in temperature, ΔT, in the weld zone due to the friction stir weld process of -200 deg F resulted in a good comparison with the measured residual stress maxima and profile. SIF solutions were generated by introducing cracks of varying length along the crack symmetry plane in the presence of residual stress using the 3D-VCCT technique [20]. The comparison of variation in the SIF solution at different values of crack length (a) for the tensile C(T) configuration is shown in Fig. 5b. The computed SIF is compared to experimental data generated using the slitting and crack compliance methods. The crack compliance data are indicated by open and filled symbols and the slitting compliance data are represented by a solid line. The SIF solution generated using the VCCT technique at various values of crack length for the tensile C(T) configuration compare well with experimental data. In order to establish the portability and applicability of the current methodology, other geometric configurations (e.g. the compressive C(T) and 4-inch wide M(T) configurations in Fig. 3) were also analyzed and compared to the experimental data. The specimens were modeled appropriately with the FSW zone and the same thermal input parameter that was previously calibrated was employed to introduce a residual stress field in the specimen. Even though the same parameters were used, each specimen has its own unique self-equilibrated residual stress field depending upon the type, geometry, and the location of the FSW. The comparison and distribution of residual stress affected SIF are shown in Fig. 6 a and b. To further test the robustness of this process, a 2% stretch was also applied to the M(T) configuration, to simulate a common processing method to alleviate residual stress. The stretch process is shown to reduce the magnitude of the residual stress and to dramatically alter the observed stress gradient (see Fig. 6c). The thermal residual stress model with a ΔT value for the applied welding process was used to model different residual stress fields for various configurations, suggesting that it can also be applied to model the residual stress distributions for complex structural configurations.

Life prediction methodology

A life prediction methodology considering the effects of residual stress on crack closure and crack tip stress ratio has been developed. Residual stress increases crack-tip mean stress without affecting applied ΔK. By carrying out crack closure analysis at an applied constant amplitude loading and stress ratio, changes in crack closure level can be determined as residual stress varies and redistributes with crack extension. A comparative plot of variation in crack opening ratio for a 4-inch wide C(T) specimen with tensile and compressive configurations as well as the crack opening for the same specimen configuration without any compressive residual stress is shown in Fig. 7. In the absence of the residual stress field, constant crack opening ratio is obtained for applied constant amplitude loading with crack extension. In contrast, the presence of a compressive or tensile residual stress field even under constant amplitude loading will vary the crack opening ratio with crack extension depending upon the type of residual stress field at the current crack tip. In addition, the residual stress field ahead of the crack tip redistributes with crack extension. As shown in Fig. 7, a compressive residual stress field ahead of the crack tip increases the crack opening ratio and a tensile residual stress decreases the opening ratio. The crack tip driving force will vary depending upon the type of residual stress ahead of the crack tip. In certain circumstances, a crack initiated at certain critical location grows through the FSW region. Under such a scenario, in addition to change in the residual stress field, the life prediction methodology also has to account for changes in material properties through the nugget, TMAZ and HAZ regions. This added level of complexity will be included in analyses to better model the residual stress distribution and to accurately model crack propagation through a representative weld microstructure.

Concluding Remarks

The residual stress field associated with the FSW process was successfully modeled using equivalent thermal loads (ΔT concept). The VCCT technique was used in generating the SIF solution and compared with experimental data for both tensile and compressive residual stress field. The same ΔT value captures the residual stress field associated with two different weld locations in C(T) specimens as well as for an M(T) specimen containing the same FSW. The equivalent thermal loads concept and its application in modeling a residual stress field in various configurations can be utilized to model the residual stress imparted in more complex geometries. A life prediction methodology has been developed to predict the life considering the effects of residual stress field and change in material property through the FSW region.

Acknowledgements

The authors would like to acknowledge the contributions of Mark James, Richard Brazill and Robert Shultz of the Alcoa Technical Center and Keith Donald and Amy Blair of Fracture Technology Associates.

References

[1] Seshadri, B.R. and Smith, S.W., "Effect of residual stress on residual strength characterization of integral structures," 12th *Joint FAA/DOD/NASA conference on aging aircraft, Kansas city, Missouri, May 4-7, 2009.*

[2] Webster, G. A. and Ezeilo, A. N., "Residual stress distributions and their influence on fatigue lifetimes," *Int. J. Fatigue*, 2001, Vol. 23(suppl 1), pp. 375–383.

[3] Nelson, D. V., "Effects of residual stress on fatigue crack propagation," *Residual Stress Effects in Fatigue*, 1982, ASTM STP 776, pp. 172–194.

[4] Wohlfahrt, H. and Lieurade, H. P., "Influence of residual stresses on the fatigue strength of welded structures," *Handbook on Residual Stresses*, 2005, Vol. 1, pp. 79–107.
[5] Zhu, X. K. and Chao, Y. J., "A Numerical simulation of transient temperature and residual stresses in friction stir welding of 304L stainless steel," *J. Mater. Process. Technol.,* 2004, Vol. 146, pp. 263–272.
[6] Parker, A. P., "Stress intensity factors, crack profiles, and fatigue crack growth rates in residual stress fields," *Residual Stress Effects in Fatigue*, 1982, ASTM STP 776, pp. 13–31.
[7] Sutton, M. A., Abdelmajid, I., Zhao, W., Wang, D. and Hubbard, C., "Weld characterization and residual stress measurement for TC-128B steel plate," *J. Press. Vess. Technol.*, 2002, Vol. 124, pp. 405-414
[8] Prime, M. B., "Measuring residual stress and the resulting stress intensity factor in compact tension specimens," *Fatigue Fract. Eng. Mater*. Vol. 22, 1999, pp. 195–204.
[9] Wu, S. and Abel, A., "Fatigue crack stress intensity factors: The influence of residual stresses. *Proceedings of the Second International Offshore and Polar Engineering Conference*," San Francisco, USA, June 1992, pp. 312–317.
[10] Ge, Y. Z., Sutton, M. A., Deng, X. and Reynolds, A. P., "Limited weld residual stress measurements in fatigue crack propagation: Part I.," *Fatigue Fract. Engng Struct.*, 2006, Vol. 29, pp. 524-536.
[11] Sutton, M. A., Reynolds, A. P., Ge, Y.Z. and Deng, X., "Limited weld residual stress measurements in fatigue crack propagation: Part II.," *Fatigue Fract. Engng Struct.*, 2006, Vol. 29, pp. 537-545.
[12] Fitzpatrick, M. E. and Lodini, A., "Analysis of residual stress using neutron and synchrotron radiation," Taylor and Francis, London, 2003, pp. 296-318.
[13] Liljdahl, C. D. M., Tan, M. L., Zanellato, O., Ganguly, S. Fitzpatrick, M. E. and Edwards, L., "Evolution of residual stresses with fatigue loading and subsequent crack growth in a welded aluminum alloy middle tension specimen," *Engng Fract. Mech.,* 2008, Vol. 75, pp. 3881-3894.
[14] Liljdahl, C. D. M., Zanellato, O., Edwards, L. and Fitzpatrick, M. E., "Evolution of residual stresses with fatigue crack growth in a variable polarity plasma arc-welded aluminum alloy compact tension specimen," *Metall. and Mater. Trans.*, 2008, Vol. 39A, pp. 2370-2377.
[15] Liljdahl, C. D. M., Brouard, J., Zanellato, O., Lin, J., Tan., M. L., Ganguly, S., Irving, P. E., Fitzpatrick, M. E., Zhang, X. and Edwards, L. "Weld residual stress effects on fatigue crack growth behavior of aluminum alloy 2024-Y351," *Int. J. of Fatig.* 2008, Vol. 39A, pp. 2370-2377.
[16] Prime, M. B., "Residual Stress Measurement by Successive Extension of a Slot: the Crack Compliance Method," *Applied Mechanics Reviews*, 1999, Vol. 52(2), pp. 75-96.
[17] Donald, J.K. and Lados, D.A., "An Integrated Methodology for Separating Closure and Residual Stress Effects from Fatigue Crack Growth Rate Data," *Fatigue and Fracture of Engineering Materials and Structures*, 2006, Vol. 30, pp. 223-230.
[18] Rybicki, E. F. and Kanninen M. F., "A finite element calculation of stress intensity factors by a modified crack closure integral," *Engng Fract. Mech*., 1977, Vol. 9, pp. 931–938.
[19] Shivakumar, K.N., Tan, P. W. and Newman Jr., J. C., "A virtual crack-closure technique for calculating stress intensity factors for cracked three dimensional bodies," *Int. J. Fract.* 1988, Vol. 36, R43–50.
[20] Shivakumar, K.N. and Newman Jr., J.C., *ZIP3D- An Elastic-Plastic Finite Element Analysis Program for Cracked Bodies, NASA TM* 102753, 1990.
[21] Rice, J. R., "*A Path Independent Integral and the Approximate Analysis of Strain Concentration by Notches and Cracks*," J. of Applied Mech. 1968, Vol. 35, pp. 379-386.

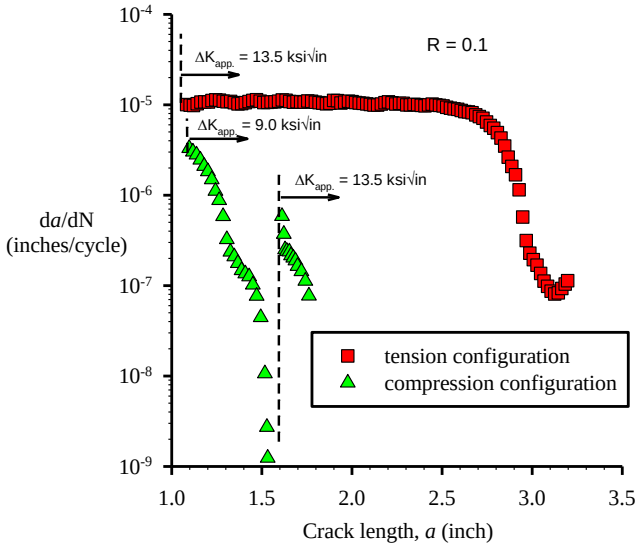

Figure 1. Fatigue crack growth rate versus crack length for Constant-DK tests of tension and compression configuration C(T) specimens.

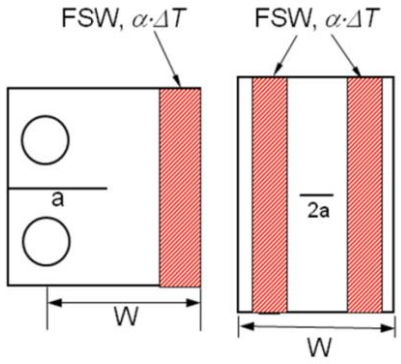

Figure 2. Configurations for computation using C(T) and M(T) specimen geometries.

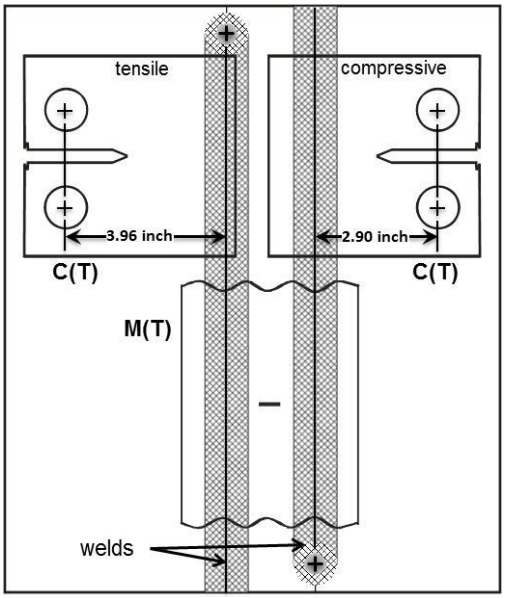

Figure 3. Schematic of the specimen configurations examined.

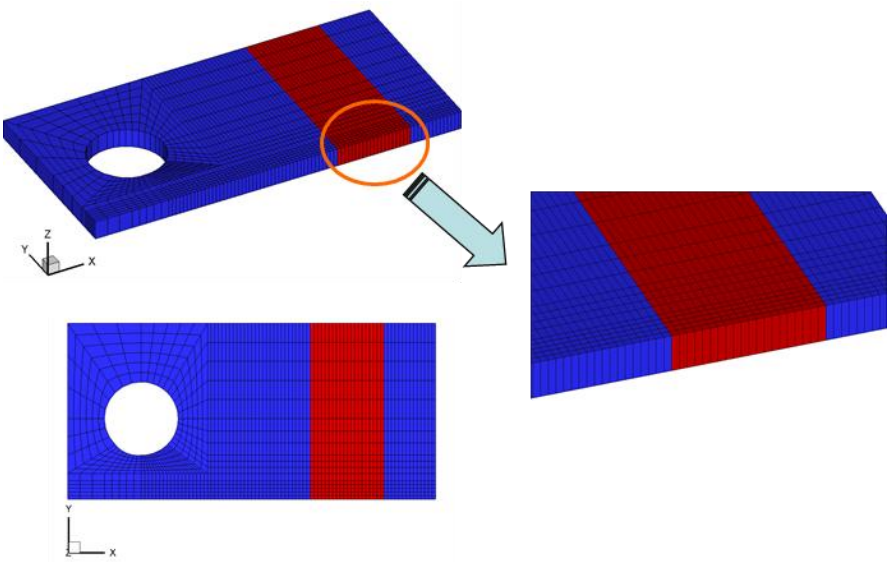

Figure 4. A typical finite element mesh for 4-inch wide C(T) specimen for residual stress analysis.

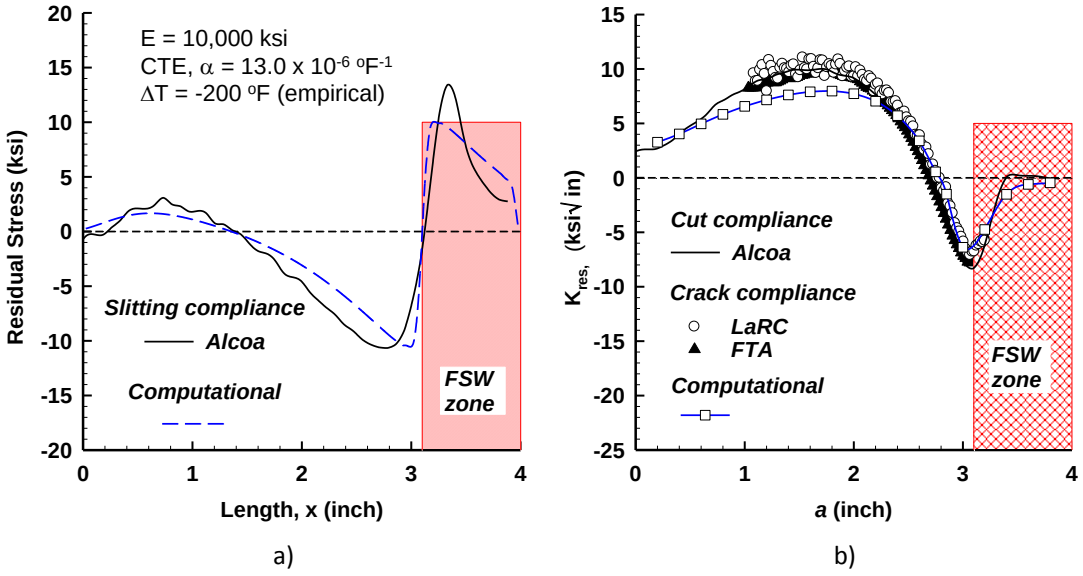

Figure 5. Variation in a) residual stress field and b) stress intensity factor along symmetry plane for 4-inch wide C(T) specimen.

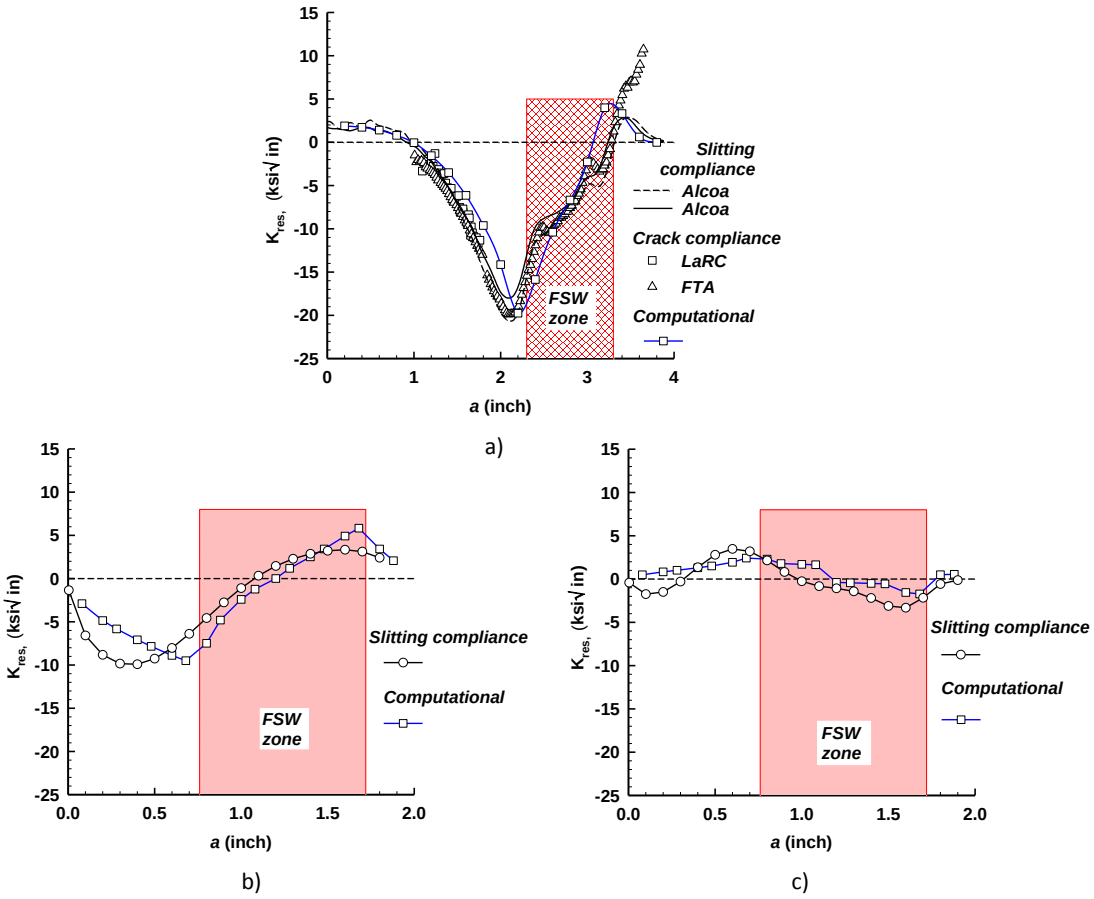

Figure 6. Stress intensity factor along symmetry plane for a) compression configuration C(T), b) 4-inch wide M(T) configuration and c) 4-inch wide M(T) with 2% tensile stretch.

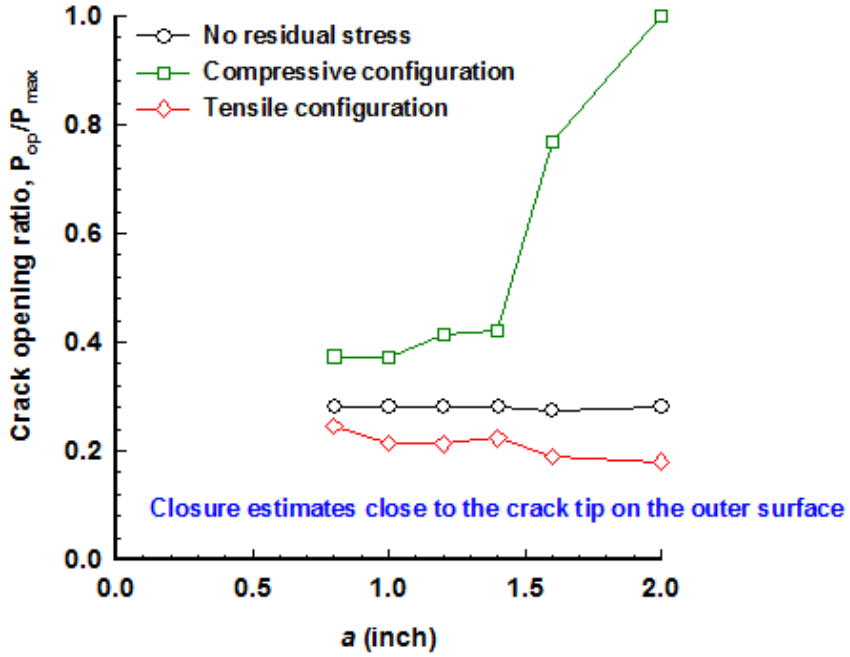

Figure 7. Variation in crack opening ratio for 4-inch wide C(T) specimen on the outer surface, tensile and compressive configurations and no residual stress.